# The Effect of Morphology and Chemical Characteristics of Cellulose Reinforcements on the Crystallinity of Polylactic Acid

**Aji P. Mathew,[1] Kristiina Oksman,[1] Mohini Sain[2]**

[1]*Department of Engineering Design and Materials, Norwegian University of Science and Technology, Trondheim, Norway*
[2]*Centre for Biocomposites and Biomaterials Processing, Faculty of Forestry and Chemical Engineering, University of Toronto, Toronto, Canada*

Received 6 July 2005; accepted 1 October 2005
Published online in Wiley InterScience (www.interscience.wiley.com).
DOI 10.1002/app.23346

**ABSTRACT:** The aim of this work has been to study the crystallization behavior of composites based on polylactic acid (PLA) and three different types of cellulose reinforcements, viz., microcrystalline cellulose (MCC), cellulose fibers (CFs), and wood flour (WF). The primary interest was to determine how the size, chemical composition, and the surface topography of cellulosic materials affect the crystallization of PLA. The studied composite materials were compounded using a twin-screw extruder and injection-molded to test samples. The content of cellulose reinforcements were 25% by weight. The MCC and WF were shown to have a better nucleating ability than CFs based on differential scanning calorimetry and optical microscopy studies. It is difficult to visualize that transcrystallization will occur during melting process and this process is influenced by the morphological and chemical characteristics of the reinforcement. Bulk crystallization seems to be mainly dependent on the processing temperature. The cold crystallization process was shown to improve the thermal stability and storage modulus of the composites. © 2006 Wiley Periodicals, Inc. J Appl Polym Sci 101: 300–310, 2006

**Key words:** biopolymer; composites; crystallization; differential scanning calorimetry; optical microscopy

## INTRODUCTION

The interest to use environmental friendly materials has had tremendous increase during the recent years, for example, car manufacturers are using natural fiber composites in both interior and exterior products. These products are usually based on different natural fibers and synthetic polymers such as polypropylene. Packaging is another product group, which needs more environmental friendly materials because of the relatively short life span of these products. Many studies have been made on potential to use natural fibers as reinforcements in different polymers while just a few studies are made on the possibility to use biopolymers as matrix in these composites.[1–5] Natural fibers, used in the applications like composites, are bundles of individual fibers held together by thin layers of polysaccharides, lignin and/or pectin. Wood and plant stems are built-up from these fiber bundles. The structure of fiber bundle is composed of different hierarchical microstructures, see Figure 1. A typical single fiber or cell has a diameter around 20–30 $\mu$m. Cell wall is composed of cellulose nanosized microfibrils and an interpenetrating matrix of hemicelluloses, and pectins and/or lignin. Again, each individual nanosized fibrils consists of both random and highly arranged structure, thereby, inducing a variable degree of crystallinity in the elementary cellulose backbone. Stiffness and the mechanical strength of these fibers are greatly influenced by their morphological structure. In general, higher the degree of crystallinity, higher is the fiber stiffness.[6,7]

In this study, the cellulose reinforcements, shown in Figure 2, are from three different levels of the hierarchical structures of wood; (1) microcrystalline cellulose (MCC), these are crystallites without lignin or hemicellulose, (2) cellulose fibers (CFs), which are individual fibers with low lignin content, and (3) wood flour (WF), which means fiber bundles bound together by lignin.

Polylactic acid (PLA) polymers or polylactides are polyesters of lactic acids and these polymers have recently been introduced commercially for products where biodegradability is wanted. PLA is a versatile polymer made from renewable agricultural raw materials, which are fermented to lactic acid. The PLA can be processed similarly as polyolefines or other thermoplastic, although the thermal stability could be better.

*Correspondence to:* K. Oksman (kristiina.oksman@ntnu.no).

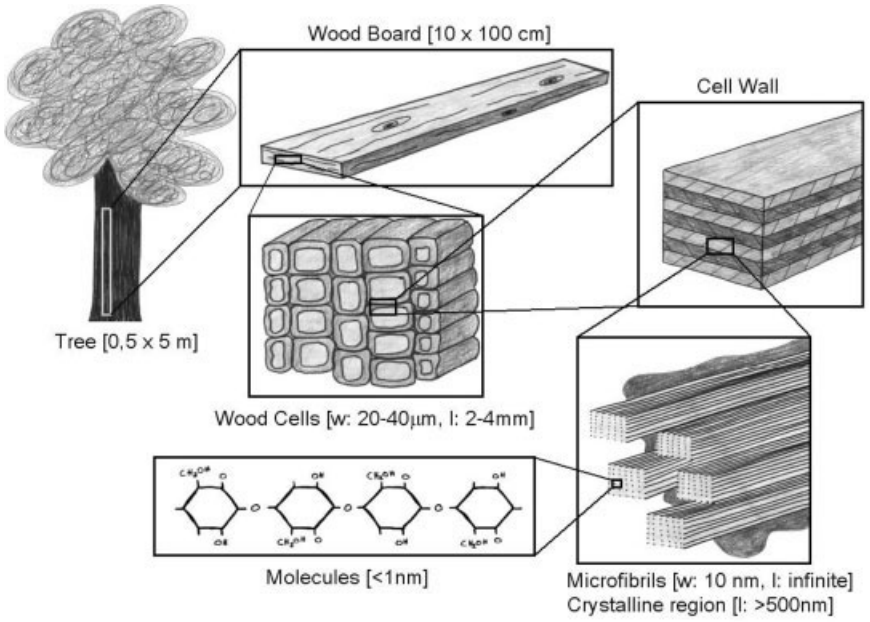


**Figure 1** The schematic of the hierarchical structure of a wood from macro to nanoscale.

Reinforcing PLA with different fibers is one possibility to improve the thermal stability of the matrix.[5]

In one of our earlier studies, we have documented that different cellulose materials (WF, CFs, and MCC) can be used as reinforcements for PLA.[8] If the polymeric matrix is crystalline in nature, then the presence of these fibers in a crystalline polymer matrix tends to influence the microstructure at the interface, and thereby the composite mechanical properties. The crystallinity of a polymeric system will depend on the processing conditions and the heating–cooling cycles that the material passes through during extrusion and injection molding steps viz, crystallization temperature, cooling rates, nucleation density, and annealing time.[9] Therefore, it is important to understand the crystallization behavior of polymer composites to explain the mechanical properties and thermal behavior of the system.

In the present study, we have focused on the crystallization of PLA in presence of these different cellulose-based reinforcements. The main objective of this work is to understand the effect of different cellulose reinforcements on the crystallization rates, crystalline structure, and morphology of PLA composites and to find possible correlations between crystallinity of the system and the morphology and properties. The crystallinity of the PLA and the composites was studied using differential scanning calorimetry (DSC) and wide angled X-ray diffraction (WAXD). The effect of cold crystallization on the dynamic mechanical thermal properties was also studied. These results on crystallinity of PLA-based composites are expected to help us in explaining the properties and performance of the different cellulose-based composites.

## EXPERIMENTAL

### Materials

#### Matrix

Poly-L-lactic acid, POLLAIT®, was supplied by Fortum Oil and Gas Oy, Porvoo, Finland. The MFI for the PLA is between 1 and 2 g/10 min (190°C, 2.16 kg). The molecular weight ($M_w$) of the PLA was 97,000 g/mol and the polydispersity was 3.2.

#### Reinforcements

Microcrystalline cellulose (MCC), cellulose fibers (CFs), and wood flour (WF) are used as the reinforcements in polylactic acid (PLA). MCC was supplied by Borregaard Chemcell, Sarpsborg, Norway. The CFs (Terracel™) were obtained from Rayonier, USA, and WF (WF, Pine) was supplied by Scandinavian Wood Fiber AB, Orsa, Sweden. These three cellulose-based reinforcements have different cellulose content, size, and surface topography. MCC is derived from high quality wood pulp by acid hydrolysis to remove amorphous regions and MCC exists as aggregates of cellulose crystallites. CFs are single fibers with high cellulose content and <2% lignin. WF used can be considered as a bundle of wood fibers consisting of cellulose, hemicelluloses, lignin, and waxes. Figure 2 shows the scanning electron micrographs of the three

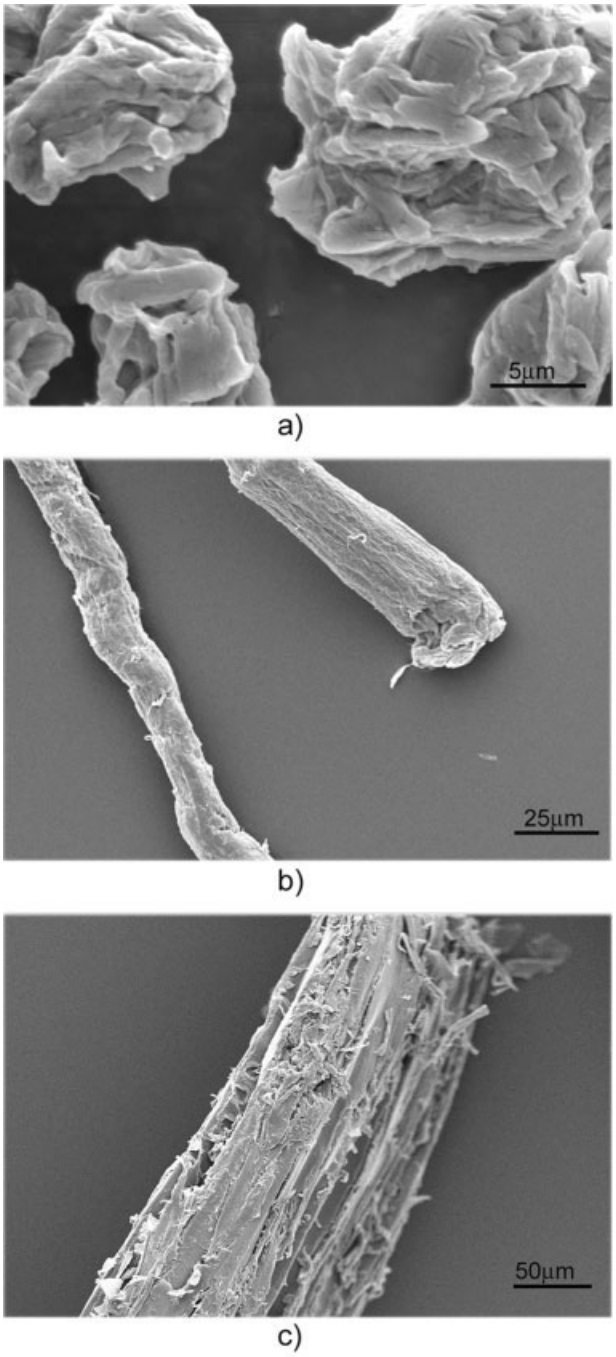


**Figure 2** Scanning electron micrographs of (a) microcrystalline cellulose (MCC), (b) cellulose fibers (CFs), and (c) wood fibers (WFs).

cellulosic materials used in this study. The physical and chemical characteristics of all the three reinforcements are summarized in Table I. It can be seen that the cellulose content is higher for CF and MCC when compared to WF.

## Processing

The composite materials were compounded using a twin-screw extruder (Coperion Werner and Pfleiderer ZSK 25 WLE) with a side feeder and gravimetric feeding systems for both main and side feeders. The processing parameters for extrusion are already described in the earlier work on PLA composites.[8] Composites were pelletized for further injection molding. Test samples were injection-molded according to ISO 294 standard for thermoplastics using Cincinnati ACT Milacron 50 injection molding machine at 200°C with a velocity of 60 mm/s. The content of MCC, CF, and WF were 25% (by weight). Pure PLA is used as the reference material in all the cases.

## Scanning electron microscopy

The morphology of used MCC, CF, and WF was studied using a scanning electron microscope (SEM), Cambridge 360, with an acceleration voltage of 10 kV. The sample surfaces were sputter-coated with Au to avoid charging.

## Heat treatment

Heat treatment of the PLA and composites were carried out to complete the cold crystallization. The samples were kept at 80°C in a hot air oven for 3 days. These samples are then tested to study the effect of cold crystallization on thermal properties, crystallinity, and dynamic mechanical properties.

## Differential scanning calorimetry

DSC experiments were carried out for pure PLA and the composites (with and without heat treatment) on a Perkin–Elmer DSC 7 calorimeter in a temperature range of 30–200°C using ~10 mg of sample specimen. All samples were tested at nonisothermal conditions at different cooling rates to study the transcrystallinity development of the matrix and to compare the nucleating ability of the reinforcements used. The experiments were carried out in five steps:

1. Heating from 30 to 200°C at a rate of 10°C/min.
2. Cooling from 200 to 30°C at a rate of 20°C/min.

**TABLE I**
**Characteristics of the Used Cellulose Materials**

| Characteristics | MCC | CF | WF |
|---|---|---|---|
| Appearance | Particles | Single fibers | Fiber Bundles |
| Particle size/diameter ($\mu$m) | 10–15 | 20–30 | 150–750 |
| Cellulose (%) | 93 | 98 | 42 |
| Lignin (%) | — | 2 | 28 |
| Hemicellulose (%) | — | — | 27 |
| Moisture (%) | 7 | — | — |
| Surface topography | Rough | Smooth | Rough |

3. Heating from 30 to 200°C at a rate of 10°C/min.
4. Cooling from 200 to 30°C at a rate of 2°C/min.
5. Heating from 30 to 200°C at a rate of 10°C/min.

The DSC studies of heat treated samples also were carried out in a temperature range of 30–200°C at a heating rate of 10°C/min. The glass transition temperature ($T_g$), melt temperature ($T_m$), cold crystallization temperature ($T_{cc}$), and heat of melting ($\Delta H_m$) are determined for all the samples and the percentage crystallinity for each curve is calculated. The percentage crystallinity of each samples is calculated using the relationship

$$X_c(\%\ \text{crystallinity}) = \frac{\Delta H_m}{\Delta H_m^{\ 0}} \times \frac{100}{w} \qquad (1)$$

$\Delta H_m$ is the enthalpy for melting, $\Delta H_m^{\ 0}$ is enthalpy of melting for a 100% crystalline PLA sample (taken as $\Delta H_m^{\ 0} = 93$ J/g), and $w$ is the weight fraction of PLA in the sample.[10,11] To determine the crystallinity of the sample, the enthalpies of cold crystallization and premelt crystallizations are subtracted from the enthalpy for melting.[12]

### Optical microscopy

Optical microscopic studies of PLA and composites were carried out to study the crystallization behavior and nucleating effect of reinforcements. Thin films of PLA and the composites with ~1% fiber content were pressed at 190°C. Four different sets of experiments were carried out at isothermal and nonisothermal conditions.

1. Isothermal melt crystallization studies: (a) Heated to 200°C in an oven and held for 5 min and (b) transferred to the microscope hot stage oven maintained at 130, 120, or 110°C.
2. Nonisothermal melt crystallization studies: (a) Heated to 200°C and held for 5 min and (b) cooled to 100°C at a cooling rate of 2°C/min.
3. Isothermal cold crystallization studies: (a) Melted at 200°C and held at that temperature for 5 min, (b) quenched using ice cold water to form amorphous polymer, and (c) transferred to the microscope hot stage oven maintained at 80°C.
4. Nonisothermal cold crystallization studies: (a) Melted at 200°C in an oven and held for 5 min, (b) quenched using ice cold water to form amorphous polymer, and (c) heated from room temperature to 100°C at 2°C/min.

### Crystallinity studies

The crystallinity of the heat-treated PLA-based composites was studied using WAXD (Siemens Diffractometer D5000). The samples were exposed for a period of 1.5 s for each angle of incidence ($\theta$) using a Cu K$\alpha$ X-ray source with a wave length ($\lambda$) of 1.541 Å. The angle of incidence is varied from 4° to 50° by steps of 0.02 s. The periodical distances ($d$) of the main peaks were calculated according to Bragg's equation ($\lambda = 2d \sin \theta$).

### Dynamic mechanical thermal analysis

The effect of heat treatment on tan $\delta$ temperature and storage modulus of different composite systems was studied by dynamic mechanical thermal analysis (DMTA Rheometrics Scientific V). DMTA was run in a dual cantilever bending mode and the typical test specimen size was $30 \times 10 \times 4$ mm$^3$. The temperature interval was from room temperature to 100°C, with a heating rate of 1.5°C/min and frequency of 1 Hz.

## RESULTS AND DISCUSSION

### Differential scanning calorimetry

#### Effect of cooling rates

Figures 3 show the thermograms and Table II gives the numerical values corresponding to PLA, PLA/MCC, PLA/CF, and PLA/WF samples obtained from the heating and cooling cycles. PLA, PLA/MCC, PLA/CF, and PLA/WF samples show glass transition and cold crystallization. In the final heating cycle as shown by curve V, all the samples show a melt peak, without glass transition and cold crystallization, indicating that the materials are highly crystalline in nature with some amorphous regions.

The $T_g$ is higher in all the composite materials compared to that of the pure PLA, showing that the polymer relaxation is delayed in the presence of reinforcements. The reason for this is the restriction of chain mobility due to increased crystallinity. It can be seen that the $T_g$ values of PLA/MCC, PLA/CF, and PLA/WF are 56.6, 57.5, and 58.3°C, respectively, where as $T_m$ remains almost constant at 175°C. The cold crystallization temperature ($T_{cc}$) values are higher for PLA compared to CF and MCC. Similar depression in $T_{cc}$ in the presence of fiber reinforcements was observed in cellulose-based PHB composites.[13] It was found that WF, MCC, and CF system crystallizes at 134, 130, and 116°C, respectively, while PLA crystallizes at 110°C. This is indicative of the nucleating ability of the reinforcements.

The heating–cooling cycles give us some information regarding the crystallinity development of cellu-

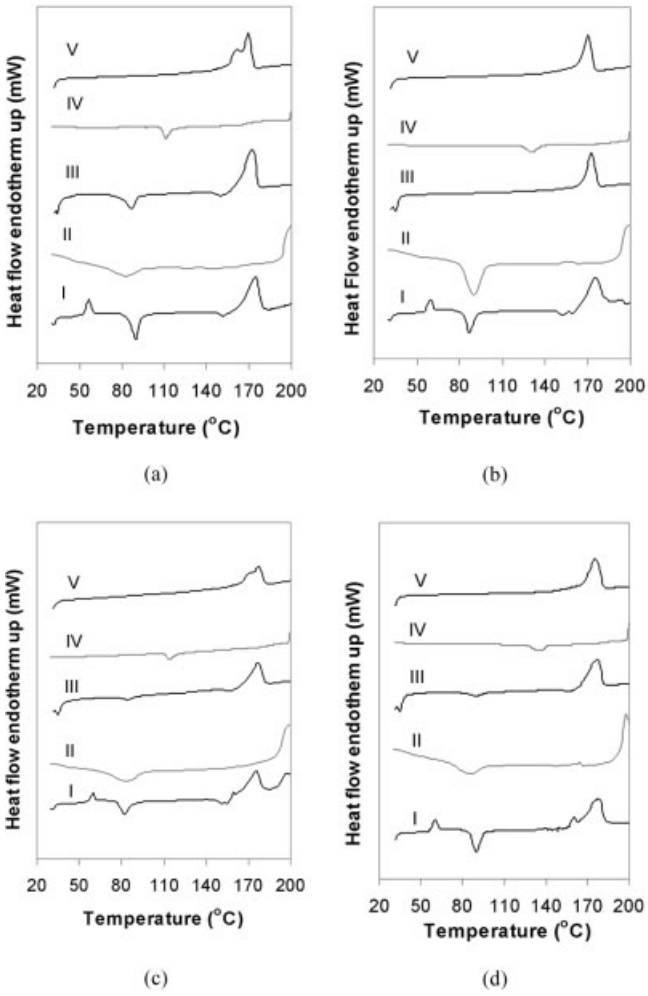


**Figure 3** DSC curves of studied materials obtained from different heating–cooling cycles: (a) PLA, (b) PLA/MCC, (c) PLA/CF, and (d) PLA/WF. I: Represents the heating from 30 to 200°C at a rate of 10°C/min; II: Cooling from melt at a rate of 20°C/min (fast cooling); III: Heating from 30 to 200°C at a rate of 10°C/min, after fast cooling; IV: Shows the cooling from melt at a rate of 2°C/min (slow cooling); V: Heating from 30 to 200°C at a rate of 10°C/min, after slow cooling.

lose-reinforced PLA. Results in Figure 3(a) show that PLA transformed into a semicrystalline polymer after a fast cooling step and, into a more crystalline polymer after a slow cooling effect. During slow cooling, the crystallinity of PLA achieved was 52%.

The crystallinity development is most marked in MCC system indicating that MCC favors nucleation and crystal growth on the surface. In the case of PLA/CF composites, the melt crystallization temperature and crystallinity is lower than for MCC and WF composites during fast and slow cooling. In the case of cellulose reinforcements, the presence of lignin is known to affect the ability of the fibers to act as nucleating agent.[14] In the present study, the lignin content is in the following order WF > CF > MCC (see Table I). However, the crystal formation does not follow the same order, indicating that the surface chemistry of the fibers is not the governing factor for the crystal formation in the studied PLA composites.

### Effect of heat treatment

Figure 4 shows the thermograms of heat-treated PLA, PLA/MCC, PLA/CF, and PLA/WF is shown for comparison. There is no transition representing glass transition or cold crystallization, indicating no detectable amorphous regions in the system. The presence of melt-peak indicates crystalline domains. The melt temperatures and the enthalpy associated with the melting are given in Table III. The melt peak is at 173°C for PLA. For the composites, the melt temperature increases in the following order: PLA/MCC < PLA/CF < PLA/WF. This indicates that the crystal sizes increases from MCC to WF system as larger crystals tend to melt at higher temperatures than the smaller crystallites.[15]

The percent crystallinity (%) is calculated using eq. (1) for all the heat-treated samples and is shown in Table III. The crystallinity is slightly higher for PLA compared to that of the composites. All composites have almost the same crystallinity. These points to the fact that, during cold crystallization, bulk crystallization predominates and transcrystalline growth may be suppressed or completely absent.

## Optical microscopy

The PLA and the composites are isothermally crystallized from the melt, at 130, 120, and 110°C, and the micrographs are shown in Figure 5. It can be seen that the spherulite size increases with increase of crystallization temperature as expected. In the case of MCC and WF composites, the nucleation and growth occurs on the reinforcement surface and transcrystallinity is observed. At higher crystallization temperature, transcrystalline growth is found to be favored, whereas at lower temperatures, both transcrystallization and bulk crystallization is observed to grow at the same rate. In the case of PLA, crystallization by self nucleation alone is possible and the crystal grows in outward direction forming spherulites. These crystals grow until they impinge on each other and further crystal growth is arrested. It was also noticed that, in the case of WF, the crystals start to grow from the defects and imperfections on the WF surface. The surface roughness in the case of MCC also is expected to favor the initiation and growth of crystals. It was not very clear from the micrographs. In the case of CF, where the fiber surfaces are smooth, the crystal formation was not initiated on the fiber surface, and mostly bulk crystallization occurred. During optical microscopy

**TABLE II**
**Thermal Characteristics of PLA and Its Composites**

| Samples | $T_g$ (°C) | $T_{cc}$ (°C) | $T_m$ (°C) | $\Delta H_m$ (J/g) | $T_{mc}$ (°C) | Crystalline % |
|---|---|---|---|---|---|---|
| *Heating at 10°C/min* | | | | | | |
| PLA | 54.1 | 90 | 175 | 43.0 | — | 19.2 |
| PLA/MCC | 56.6 | 86.6 | 175.8 | 48.0 | — | 44.5 |
| PLA/CF | 57.5 | 82.5 | 175 | 40.5 | — | 35.3 |
| PLA/WF | 58.3 | 90 | 175.8 | 49.5 | — | 45.0 |
| *Fast cooling at 20°C/min* | | | | | | |
| PLA | — | — | — | — | 83.3 | — |
| PLA/MCC | — | — | — | — | 89.9 | — |
| PLA/CF | — | — | — | — | 83.3 | — |
| PLA/WF | — | — | — | — | 84.9 | — |
| *Heating after cooling at 20°C/min* | | | | | | |
| PLA | — | 86.7 | 171.7 | 47.9 | — | 32.0 |
| PLA/MCC | — | — | 173.4 | 34.6 | — | 49.0 |
| PLA/CF | — | 85 | 176.7 | 32.2 | — | 36.1 |
| PLA/WF | — | 90 | 176.7 | 35.7 | — | 38.0 |
| *Cooling at 2°C/min* | | | | | | |
| PLA | — | — | — | — | 111.3 | — |
| PLA/MCC | — | — | — | — | 130.9 | — |
| PLA/CF | — | — | — | — | 114.3 | — |
| PLA/WF | — | — | — | — | 135.5 | — |
| *Heating after cooling at 2°C/min* | | | | | | |
| PLA | — | — | 170.0 | 48.8 | — | 52.6 |
| PLA/MCC | — | — | 170.0 | 46.2 | — | 66.3 |
| PLA/CF | — | — | 178.3 | 33.6 | — | 48.3 |
| PLA/WF | — | — | 175.9 | 42.0 | — | 60.3 |

$T_g$, glass-transition temperature; $T_{cc}$, cold crystallization temperature; $T_m$, melt temperature; $T_{mc}$, melt crystallization temperature; $\Delta H_m$, heat of fusion.

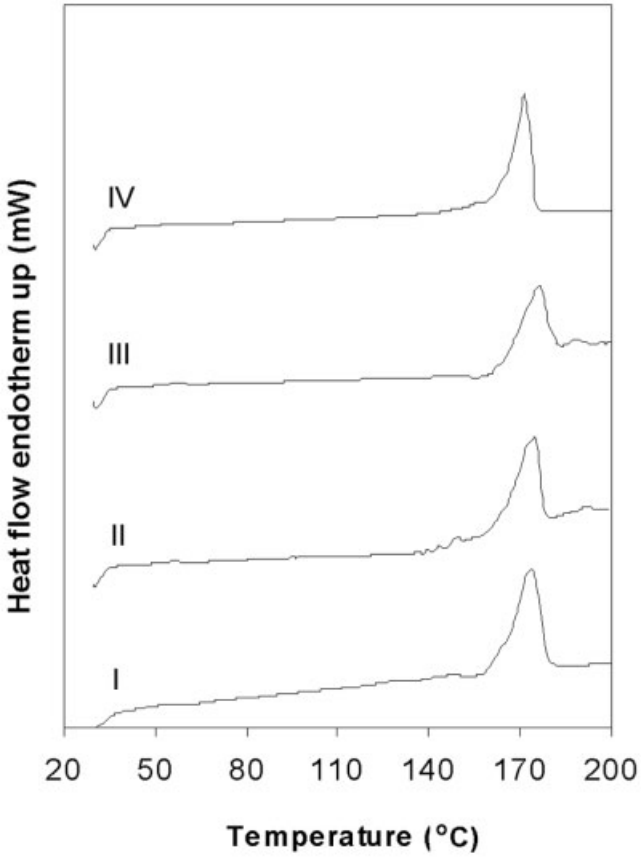


**Figure 4** DSC curves for heat-treated (I) PLA, (II) PLA/CF (III) PLA/WF, and (IV) PLA/MCC composites.

studies, the PLA showed a tendency to nucleate on CF where there are defects due to bending or crushing of fibers. This leads to the conclusion that, in the case of composites, the surface topography plays a significant role in the nucleation capability of the cellulosic reinforcements.

Micrographs of the crystal structure for PLA and its composites during nonisothermal crystallization from the melt are shown in Figure 6. PLA shows crystal growth in the bulk around 120°C and the crystals develop rapidly around 110°C. The figure shows that, in WF system, spherulite formation is initiated from the reinforcement surface. The MCC also showed some tendency to initiate crystal growth though bulk crystallinity also seemed to develop simultaneously. In the CF samples, the crystal growth was observed on the fibers where there were defects or imperfections and the bulk crystallinity seems to be favored than transcrystallinity. The micrographs taken at 110°C also reflect the same trend.

The transcrystalline growth was observed and the bulk crystallization was found to be diminished in MCC and WF composites. The samples were prepared with very few reinforcing particles, so as to view the crystal initiation and growth clearly. Therefore, we can expect that in the true composite, especially in MCC and WF composites, where the number of reinforcing entities is higher and the distance between the

**TABLE III**
**Thermal Characteristics of PLA and Composites after Heat Treatment**

| Samples | $T_g$ (°C) | $T_{cc}$ (°C) | $T_m$ (°C) | $\Delta H_m$ (J/g) | Crystallinity DSC (%) | Crystallinity WAXD (%) |
|---|---|---|---|---|---|---|
| HT-PLA | No | No | 173.3 | 53.5 | 57.5 | 49.8 |
| HT-PLA/MCC | No | No | 171.6 | 39.3 | 56.5 | 49.6 |
| HT-PLA/CF | No | No | 174.2 | 37.2 | 53.4 | 52.5 |
| HT-PLA/WF | No | No | 175.8 | 36.6 | 52.5 | 47.0 |

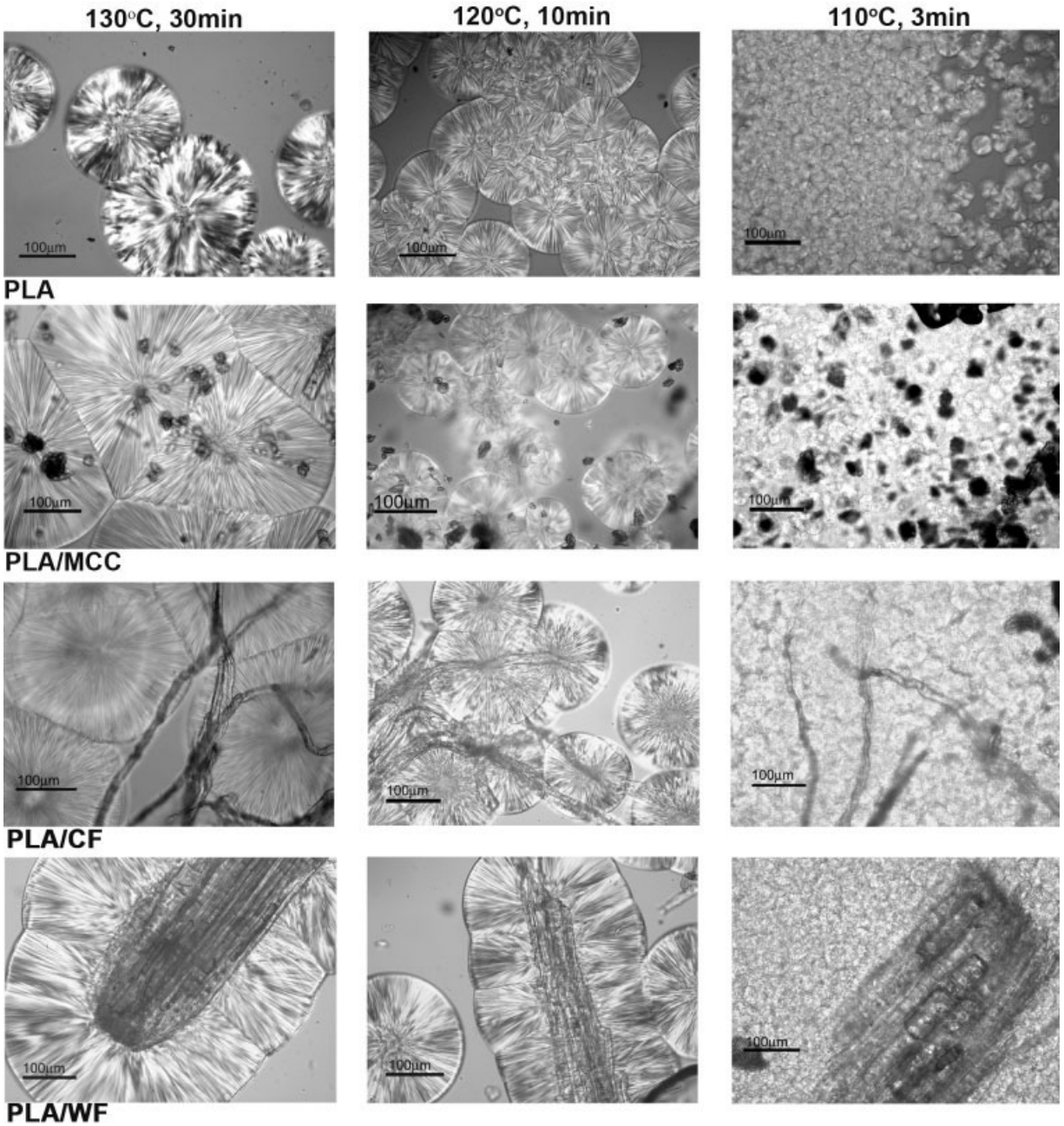


**Figure 5** Optical micrographs of PLA and composites during isothermal melt crystallization.

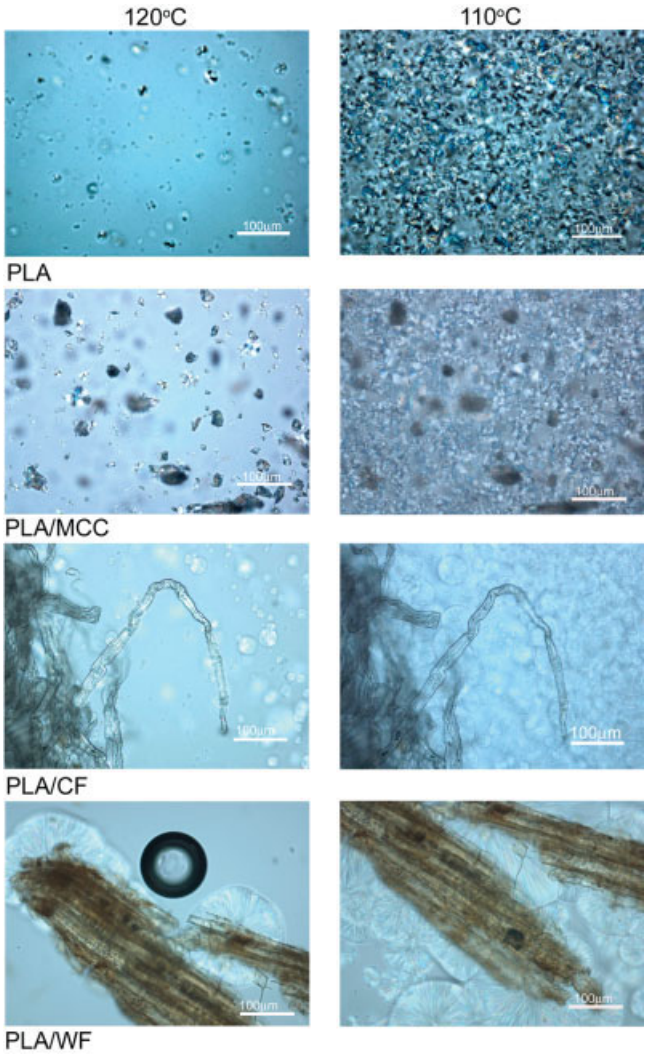


**Figure 6** Optical micrographs of PLA and composites during nonisothermal melt crystallization. [Color figure can be viewed in the online issue, which is available at www.interscience.wiley.com.]

reinforcements are short, trascrystallinity occurs predominantly. Moon[16] has pointed out that the formation of transcrystalline structure in fiber-reinforced semicrystalline thermoplastic matrix like PP impedes the spherulite formation and development in the matrix phase. He also found that, in composites with high fiber volume fraction, transcrystallinity occurs in the interface and spherulites will not have space for formation and growth. This is applicable in systems with large fiber surface area like MCC and the large number of nucleating sites can lead to the formation of crystals, which impinge on each other resulting in large number of small crystal domains. In PLA/CF composites, limited transcrystallinity is expected to develop defects or imperfections, resulting in a predominantly bulk crystalline morphology. Another factor that needs to be considered while explaining the crystallinity development in the composites is the sample thickness. The true composites are thicker than the test specimens used for the optical microscopy studies and the different layers of the composite tend to cool down at different rates. The temperature will be higher and cooling rates will be slower as the distance from the surface increases, which may lead to a corresponding increase in spherulite size.

PLA and composites are cold crystallized nonisothermally by heating amorphous samples from room temperature to 100°C. All the systems showed similar crystalline structure, Figure 7 shows the typical morphology with small crystallites PLA/CF composites. In all the samples, the matrix is crystalline and it consists of small crystallites and the crystal size was found to be independent of the nature of the nucleating agents present. This confirms the fact that, during cold crystallization, the crystals develop by bulk crystallization.

### Wide angled X-ray diffraction

Figure 8 shows the diffraction pattern of PLA before and after heat treatment. Untreated PLA exhibited very low crystallinity and exhibited a single peak at about $2\theta = 16.4°$ and a broad hump showing amorphous nature. It can be seen that, after heat treatment, the diffraction pattern is indicative of a crystalline material and shows peaks at $2\theta = 16.4°$ and 19.1°. Further the hump has disappeared showing that amorphous chains have been rearranged to crystalline regions. Figure 9 shows the diffraction patterns of PLA/MCC25, PLA/CF25, and PLA/WF25 systems after cold crystallization. In all the cases, the peaks at $2\theta = 16.4°$ and 19.1° are highly prominent indicating a

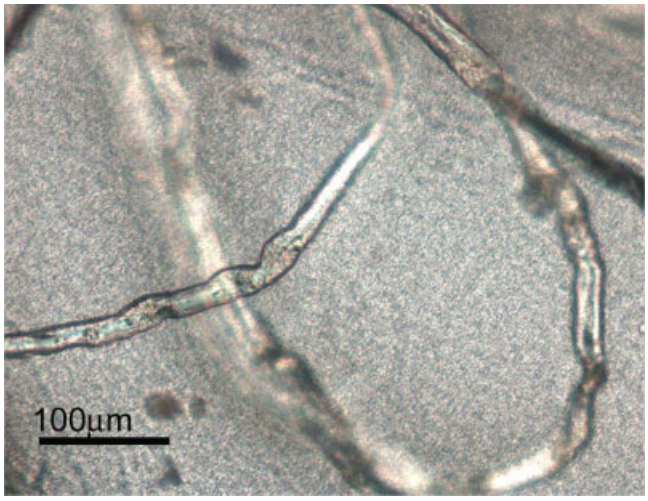


**Figure 7** Typical microstructure of cold-crystallized PLA composite. [Color figure can be viewed in the online issue, which is available at www.interscience.wiley.com.]

crystalline PLA matrix. The peak observed at $2\theta = 22.4°$ is from cellulose. The other peaks for cellulose are ill-defined as they are masked by the high intensity of PLA peaks. The diffraction patterns of the cold-crystallized samples were compared with those without heat treatment, which is reported in our earlier study.[8] It can be seen that, after heat treatment, the diffraction patterns are very much different and indicative of crystallinity, with well-defined peaks corresponding to PLA as well as cellulose. The percent crystallinity of these cold-crystallized samples was calculated based on X-ray analysis and they are given in Table III. It can be seen that the crystallinity of PLA and the composites are very similar. Further, the crystallinity values of the composites did not show any regular trend depending on the nature of reinforcements confirming our microscopy results that cold crystallization occurs independent of the nucleating ability of the reinforcements. It can be seen that the crystallinity of PLA and the composites are very similar. Further, the crystallinity values of the composites did not show any regular trend depending on the nature of reinforcements confirming our inferences from microscopy results that cold crystallization occurs independent of the nucleating ability of the reinforcements.

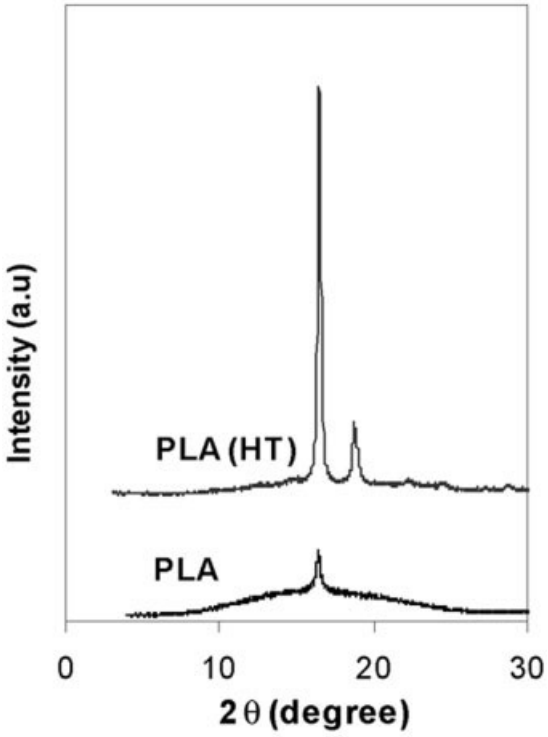


**Figure 8** Comparison of the crystallinity of PLA before and after heat treatment using WAXD.

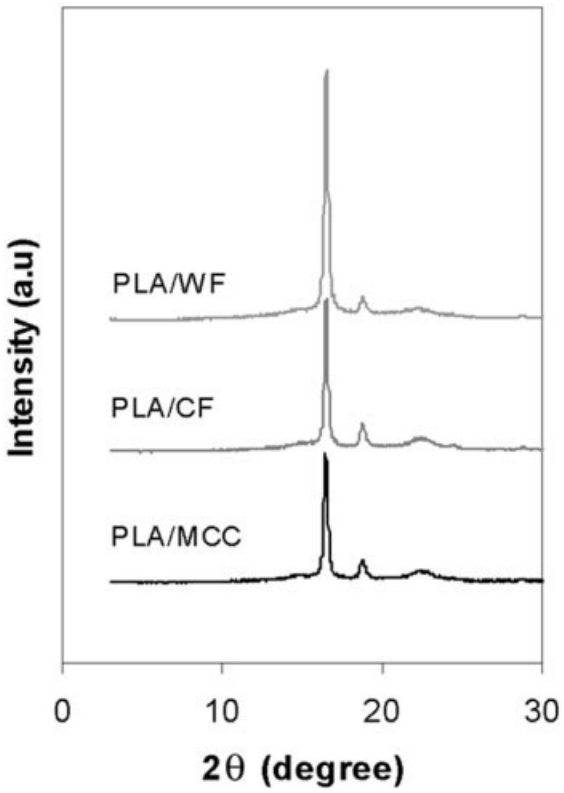


**Figure 9** Comparison of crystallinity of heat-treated composites using WAXD.

### Dynamic mechanical thermal analysis

The dynamic mechanical tests were done to study the effect of cold crystallization on the dynamic mechanical performance of pure PLA and its composites. PLA is a semicrystalline polymer but it is usually amorphous, because the crystallization occurs at temperatures around 80°C. Figure 10 shows dynamic modulus and tan δ curves of heat-treated PLA and its composites, the untreated PLA is also shown for comparison. For untreated PLA, the tan δ peak is observed around 66°C, but for heat-treated samples, this peak is almost absent. The tan δ peak intensity is indicative of the number of polymer chains involved in the relaxation process. Since the peak is almost absent, it can be concluded that amorphous regions capable of $\alpha$-relaxation is not detectable in the system. This is due to the cold crystallization that had taken place during heat treatment, resulting in the crystallization of the amorphous regions. The heat treatment is not expected to result in 100% crystallinity, but the crystalline regions might restrict the chain mobility. Figure 10 also shows the dynamic modulus of heat-treated PLA and the composites compared with untreated PLA. Here also it can be seen that, unlike pure PLA, there is no sharp decrease in modulus corresponding to $\alpha$-relaxation of amorphous regions. It is also possible to see that the

modulus start to increase after 80°C for the untreated PLA, this is a typical effect of cold crystallization.[17] The dynamic modulus was found to increase appreciably by heat-treating the PLA and its composites, see also Table IV. The samples did not exhibit any softening even at 100°C. As PLA is an unique biodegradable polymer with very promising applications, any improvement in thermal stability is highly significant. Therefore, heat treatment can be considered as a possible way to improve the thermal stability of PLA and PLA-based composites.

**TABLE IV**
**Dynamic Modulus of PLA and Composites after and before Heat Treatment**

| | Dynamic modulus at 80°C | |
|---|---|---|
| Materials | Heat-treated ($10^6$ Pa) | Untreated ($10^6$ Pa) |
| PLA | 720 | 2.15 |
| PLA/MCC | 1610 | 8.45 |
| PLA/CF | 2160 | 46.7 |
| PLA/WF | 2150 | 24.5 |

## CONCLUSIONS

This study has been focused on the crystallization behavior of PLA in the presence of three different cellulose-based reinforcements, viz, MCC, CFs, and WF. Differential scanning calorimetric studies of PLA and the composites showed that melt crystallization temperature ($T_{mc}$) and crystallinity (%) was higher for MCC and WF showing that these cellulose materials have higher capacity to act as nucleating agents compared to CF. All materials showed a semicrystalline nature initially and, after cold crystallization, the results indicated a highly crystalline system.

The optical microscopic studies were carried out for PLA and the composites to study the crystal growth during melt crystallization as well as cold crystallization. It was found that crystallization temperature influences the size and number of spherulites formed and higher temperature resulted in bigger spherulite. MCC and WF showed higher tendency to develop transcrystallinity and pure PLA as well as CF system showed bulk crystallization. CF showed the least nucleating ability and the transcrytallinity is not favored. This behavior can be attributed to the surface topography of the fiber. The results from the optical microscopy are in agreement with the DSC results. The X-ray diffraction studies also indicated a highly crystalline system after heat treatment.

The DMTA study showed that the change of matrix crystallinity by heat treatment improved the dynamic modulus and thermal stability considerably and can be considered as a possible method to increase the thermal properties of the composite.

The differences in the nucleating ability of the three cellulosic materials lead to the conclusion that in these PLA composites, the surface topography of the fiber and not the chemical composition is the decisive factor on crystallinity development. In the actual composites, where the distances between the reinforcing entities are small, it is expected that transcrystallization occurs completely and growth of crystals in the bulk is suppressed, especially for MCC composites. Also, in the composites, the different layers will cool down at different rates and larger spherulites may develop in the inner regions compared to the surface. The cold crystallization was found to be unaffected by the nature and presence of reinforcements and was occurring by development of large number of small crystallites in the bulk.

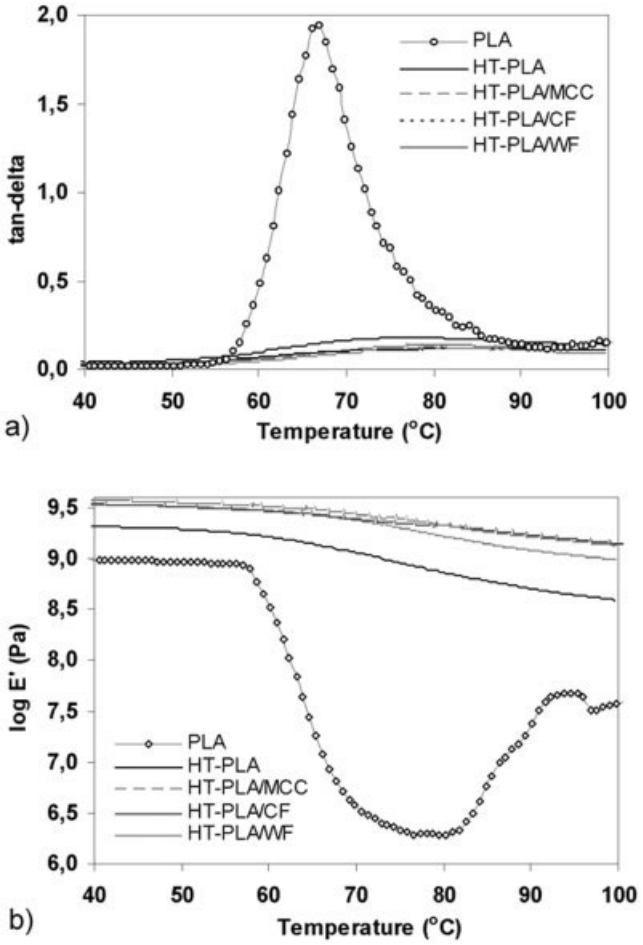


**Figure 10** DMTA curves for PLA, PLA/MCC, PLA/CF, and PLA/WF composites; (a) tan δ and (b) dynamic modulus.

The authors thank Fortum Oil and Gas Oy, Finland; Borregaard Chemcell, Norway; Scandinavian Wood Fiber AB, Sweden; and Rayonier, USA for supplying the materials.

## References


1. Sanadi, A. R.; Cauldfield, D. F.; Rowell, R. Plast Eng 1994, 4, 27.
2. Bledzki, A. K.; Riehmane, S.; Gassan, J. J Appl Polym Sci 1996, 5, 1329.
3. Oksman, K.; Wallstrom, L.; Berglund, L. A.; Filho, R. D. T. J Appl Polym Sci 2002, 84, 2358.
4. Riedel, U.; Nickel, J. Angew Makromol Chem 1999, 272, 34.
5. Oksman, K.; Skrifvars, M.; Selin, J.-F. Compos Sci Technol 2003, 63, 1317.
6. Page, D. H.; El-Hosseiny, F.; Winkler, K. Nature 1971, 229, 252.
7. Bos, H. L.; Van Den Oever, M. J. A.; Peters, O. C. J. J. J Mater Sci 2002, 37, 1683.
8. Mathew, A. P.; Oksman, K.; Sain, M.; J Appl Polym Sci 2005, 97, 2014.
9. Schulz, E.; Kalinka, G.; Auersch, W. J Macromol Sci Phys 1996, B35(3/4), 527.
10. Vasanthakumari, R.; Pennings, A. J. Polymer 1983, 24, 175.
11. Reinsch, V. E.; Kelley, S. S. J Appl Polym Sci 1997, 64, 1785.
12. Nam, J. Y.; Ray, S. S.; Okamoto, M. Macromolecules 2003, 36, 7126.
13. Reinsch, V. E.; Kelley, S. S. J Appl Polym Sci 1997, 64, 1785.
14. Baillie, C. A.; Zafeiropoulos, N.; Mwaikambo, L. Y.; Ansell, M. P.; Dufresne, A.; Entwistle, K. M.; Herrera-Franco, P. J.; Escamilla, G. C.; Groom, L.; Hughes, M.; Hill, C.; Rials, T. G.; Wild, P. M. J Mater Sci 2001, 36, 2107.
15. Angles, N.; Dufresne, A. Macromolecules 2000, 33, 8344.
16. Moon, C. K. J Appl Polym Sci 1998, 67, 1191.
17. Chartoff, R. P. In Thermal Characterization of Polymeric Materials, 2nd ed.; Turi, E. A., Ed.; Academic Press: New York, 1997; Vol. 1, Chapter 3.